Journal of Materials Chemistry B

Accepted Manuscript

ROYAL SOCIETY OF CHEMISTRY

www.rsc.org/materialsB

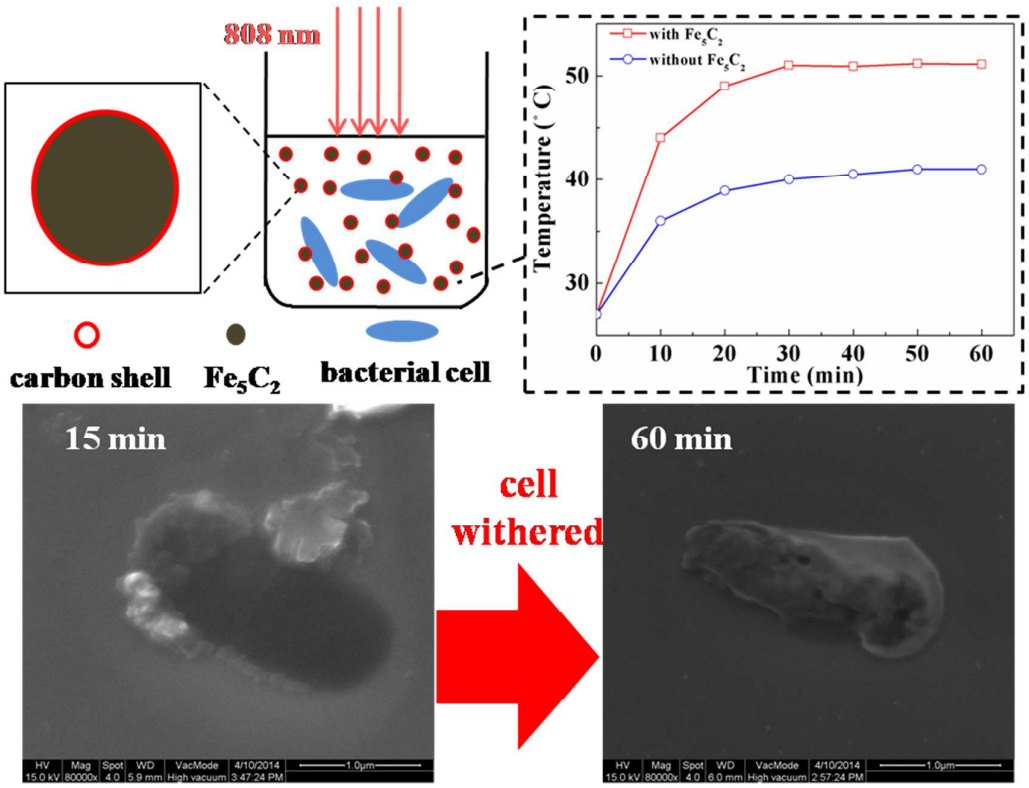

Journal of Materials Chemistry B

RSCPublishing

ARTICLE

Fe_5C_2 nanoparticles: a reusable bactericidal material with photothermal effect under near-infrared irradiation

Cite this: DOI: 10.1039/x0xx00000x

Received 00th February 2015,
Accepted 00th February 2015

DOI: 10.1039/x0xx00000x

www.rsc.org/

Yinjia Jin [a, b], Jun Deng [a], Jing Yu[c], Ce Yang[c], Meiping Tong[* a] and Yanglong Hou[*c]

Hägg iron carbide (Fe_5C_2) was synthesized through a facile one-pot wet-chemical route and employed as a photothermal agent to inactivate bacterial cells. The as-prepared Fe_5C_2 nanoparticles (NPs) were about 20 nm in diameter, and contained strong magnetic property (Ms=122 emu/g at 298 K). Fe_5C_2 NPs exhibited excellent antibacterial capability toward both Gram-negative *Escherichia coli* (*E. coli*) and Gram-positive *Staphylococcus aureus* (*S. aureus*) under near-infrared (NIR) irradiation. Under NIR irradiation, complete inactivation of *E. coli* and *S. aureus* cells (about 2×10^6 CFU/mL) could be obtained by 50 mg/L Fe_5C_2 NPs in 60 min and 150 min, respectively. Humic acid (HA) slightly inhibited the disinfection efficiency of Fe_5C_2 NPs, however, more than 99.9% of E. coli cells were inactivated in 60 min even when the concentration of HA was as high as 10 mg/L. Complete disinfection of *E. coli* cells could be achieved with the presence of 10 mg/L HA by increasing reaction time to 90 min. Moreover, Fe_5C_2 NPs showed great reusability, and complete disinfection of *E. coli* cells remained even after five consecutive reuse cycles. The increase in temperature of bacterial suspension caused by the photothermal effect of Fe_5C_2 NPs was determined to be the main reason for the inactivation of bacteria. Our study showed Fe_5C_2 NPs have great application potential for bacterial disinfection in water.

Introduction

Waterborne pathogens, including a variety of helminthes, protozoa, fungi, bacteria, rickettsiae, viruses and prions, have a devastating effect on public health and cause millions of deaths every year [1, 2]. Free chlorine, chloramines and ozone are the commonly used as chemical disinfectants to inhibit microbial pathogens. However, these chemicals can react with various constituents in natural waters to form more than 600 kinds of disinfection byproducts (DBPs), many of which are carcinogens [3, 4]. Although ultraviolet (UV) light has also been widely used in medical disinfection, the hazards of intensive and direct use of UV radiation has hindered its usage in large scale drinking water sterilization [2, 5]. Moreover, with the increasing use of numerous antibiotics, many bacterial strains have been found to be multiple-drug-resistant, causing severe infections worldwide [6, 7]. Hence, the exploration of new water pretreatment methods to control and eradicate pathogen microorganisms is of great importance.

Different types of nanomaterials (chitosan, TiO_2, ZnO, Ag, carbon nanotubes, fullerenes, etc) have been demonstrated to contain bactericidal properties and have application potential for water disinfection [4, 8-13]. For example, Bao et al. [9] reported that Ag NPs modified graphene oxide could efficiently inactivate both of Gram-positive and Gram-negative bacteria cells. Liu et al. [10] found that Ag/TiO_2 nanofiber membrane could inactivate more than 99.9% of bacterial cells under solar light. Very recently, Li et al. [13] found that 100% mortality of GFP-expressing *E. coli* cells could be achieved by exposing to 100 mg/L ZnO NPs under 4 h UV-365 light irradiation. However, these nanomaterials would be difficult to separate from water completely after use due to their small sizes. Whereas, magnetic nanoparticles (MNPs), which can be conveniently separated from water by the employment of magnetic process, have been used for water disinfection after functionalized with different materials [14-20] For example, Chen and Chen [16] modified Fe_3O_4 nanoparticles with TiO_2 and found the fabricated Fe_3O_4/TiO_2 core/shell composites exhibited great bactericidal capacity under UV light. By encapsulation of magnetite particles with poly (hexamethylene biguanide), Bromberg et al. [17] showed the synthesized core-shell paramagnetic nanoparticles possessed a large range bactericidal activity. Fe_5C_2 NPs with a thin carbon shell coating, which contain stronger saturation magnetization (~140 emu/g) [21] relative to magnetite nanoparticles (~70 emu/g) [22], can be fabricated by using a facile bromide induced synthetic method. Previous studies have shown that carbon materials, such as carbon nanotubes [23, 24] and graphene [25], could convert light energy into heat to destruct cells due to the photothermal effect. With carbon shell, Fe_5C_2 NPs might also have photothermal effect and possess antibacterial property. However, to the best of our knowledge, the bacterial disinfection property of Fe_5C_2 NPs has not been explored.

Herein, the objective of this study is to fabricate Fe_5C_2 NPs and investigate their antibacterial property. Two representative

bacterial types: Gram-negative *E. coli* and Gram-positive *S. aureus*, were utilized as model cells. The antibacterial effects of Fe_5C_2 NPs for both cell types were determined under NIR irradiation. The mechanisms involved in the disinfection processes of Fe_5C_2 NPs were discussed and proposed. The influence of natural organic matter (NOM) on the antibacterial effect was also studied. Moreover, recovery and reusability of Fe_5C_2 NPs were examined through five consecutive bacteria disinfection cycles.

Experimental section

Chemicals

Cetyltrimethylammonium bromide (CTAB), sodium dodecyl benzene sulfonate (SDS) and Octadecylamine were purchased from China National Medicines Corporation Ltd. Pentacarbonyl iron $Fe(CO)_5$ and 1-diazo-2-naphthol-4-sulfonic acid were purchased from Alfa Aesar Company.

Synthesis

Fe_5C_2 NPs were synthesized with a classic hot injection strategy, during which octadecylamine was utilized as both of solvent and surfactant, while cetyltrimethylammonium bromide (CTAB) and $Fe(CO)_5$ were used as inducing agent and precursor, respectively. Octadecylamine (14.5 g) and CTAB (0.113 g) were mixed in a four-neck flask and degassed under a flow of high purity N_2. The mixture was heated to 393 K, and then 0.5 mL of $Fe(CO)_5$ (5% in hexane) was injected into the mixture under a N_2 blanket. Following that, the mixture was heated to 453 K at 10 K/min and kept at this temperature for 10 min. The color of the mixture gradually changed from orange to black, implying the decomposition of $Fe(CO)_5$ and the nucleation of Fe nanocrystals. Subsequently, the mixture was further heated to 623 K at 10 K/min and kept there for 10 min and then cooled to room temperature. After separated with a magnet, the product was washed with ethanol and hexane, then collected for a further hydrophilic treatment. 15 mg of the as-synthesized product was dispersed in 1% sodium dodecyl benzene sulfonate (SDS) solution, and 40 mg of 1-diazo-2-naphthol-4-sulfonic acid was added into the SDS solution. After an ultrasonification process, the mixture was stirred for 15 min, washed with hexane, water, and acetone in sequence to remove the residual unreacted substrates. The as-synthesized NPs were dispersed in degassed water and kept in an Ar-filled glovebox to avoid exposure to air for further use.

Characterization methods

Transmission electron microscopy (TEM, FEI Tecnai T20, USA) was used to verify the morphology of the NPs, while high-resolution TEM (HRTEM, FEI Tecnai F20) was employed to observe the lattice spacing in the NPs. X-ray diffraction (XRD) patterns were recorded to confirm the component of the NPs using a Rigaku DMAX-2400 X-ray diffractometer equipped with Cu Kα radiation. X-ray photoelectron spectroscopy (XPS) measurements were carried out on an Axis Ultra imaging photoelectron spectrometer (Kratos Analytical Ltd.) to further verify the chemical constitution of the NPs. Raman spectroscopy (Renishaw 1000 Raman imaging microscope system) and Fourier transform IR spectroscopy (FTIR, Nicolet Magna-IR 750) were carried out to clarify the surface characterization of the NPs. The magnetic property of the as-synthesized NPs was investigated using a superconducting quantum interference device (SQUID, MPMSXL-7 Tesla, Quantum Design, USA). The optical absorption of the NPs was investigated using a UV-vis-NIR solid-state spectrometer (SolidSpec-3700/3700DUV, Shimadzu, Japan). Environmental scanning electron microscopic (ESEM, FEI Quanta 200 FEG) was used to observe the changes of bacterial morphology during the inactivation reaction.

Bacteria preparation

E. coli and *S. aureus*, which have been widely used as Gram-negative and Gram-positive model bacteria, were employed in this research as model bacterial cells. Both of *E. coli* and *S. aureus* were grown in 150 mL autoclaved flasks containing 100 mL of Luria Broth growth medium, consisting of 10 g/L tryptone, 5 g/L bacto-yeast extract, and 10 g/L NaCl. The flasks were shaken at 150 rpm in a shaker incubator under 37 °C until the early stationary phase was reached (16 h for *E.coli* and 40 h for *S. aureus*, OD600 were about 1.7). Cells were then separated by centrifugation (4000 × *g* for 10 min at 4 °C). After the centrifugation, the bacterial pellets were washed three times with sterilized physiological saline (0.9% of NaCl at pH 7.0) to remove any residual growth medium. The bacterial pellets were then re-suspended in proper volume of sterilized physiological saline to obtain the bacterial stock solutions with cell densities of approximately 2×10^8 colony forming unit (CFU) per mL.

Photothermal antibacterial tests

The photothermal antibacterial experiments were conducted in a 10-mL transparent glass bottle. Bacterial cells were suspended in the glass bottle containing 4.5 mL of sterilized physiological saline and then 0.5 mL of Fe_5C_2 NPs suspension was added into the saline. The concentrations of bacterial cells and Fe_5C_2 were controlled at 2×10^6 CFU/mL and 50 mg/L, respectively. The glass bottle was then placed under NIR laser irradiation (808 nm, 2.5 W/cm^2) at a distance of 7 cm. At different time intervals, 100 μL of bacteria-NPs mixture was sampled, diluted, and measured for surviving bacterial concentration using the plate count method [26]. Control experiment was carried out with 5 mL of bacteria suspension (2×10^6 CFU/mL) in the absence of Fe_5C_2 NPs both with and without NIR laser irradiation. Suwannee River humic acid (SRHA) (Cat#2S101H, Standard II, International Humic Substances Society), which has been previously used as model NOM [27], was employed to model humic substances. The effect of HA on the disinfection property of Fe_5C_2 NPs under NIR was investigated by adding different amounts of HA to the bacterial suspensions. For the material reusability test, the antibacterial experiment was repeated five cycles consecutively. After each cycle, a magnet was placed on the sidewall of the bottle to ensure the NPs were not decanted with the saline. Then fresh bacteria suspension was added into the bottle to conduct the next cycle of antibacterial experiment. It should be noted that each set of the experiments was performed in triplicate.

Results and discussion

Characterization of materials

XRD spectra of NPs was recorded and presented in Fig. S1, ESI †. The characteristic peaks observed in the XRD spectra of fabricated material were consistent with those observed in Fe_5C_2 spectra (JCPDS no. 36-1248), indicating that the fabricated material contained Fe_5C_2. The size and morphology of NPs were characterized by both TEM and HRTEM (Fig. 1). TEM image shows that the fabricated NPs were about 20 nm in diameter, which is consistent with the average particle size estimated from the Scherrer equation (23.1 nm). Whereas, after dispersed in water, the size of the Fe_5C_2 nanoparticles determined by Zetasizer Nano ZS90 (Malvern Instruments, U.K) was found to be about 50 nm due to aggregation. The aggregation of nanoparticles in water has been frequently reported in other studies [28, 29]. HRTEM image reveals that the prepared NP contains a core-shell structure. The lattice spacing in the core was found to be 0.205 nm, which

corresponded to the (510) plane of Fe_5C_2 [21]. Since an amorphous shell was observed in the core-shell structure of Fe_5C_2 NPs, the nature of the shell was investigated with both XPS and Raman spectroscopy. XPS spectroscopy (Fig. S2, ESI †) shows that the fabricated NPs contain C, O, and Fe, and the percentage of these elements were 70.55%, 18.27, and 9.66%, respectively. The two peaks at 710 and 724 eV observed in the Fe 2p spectrum (Fig. S3 a, ESI †) could be assigned to Fe_3O_4, whereas the two peaks at 707 and 721 eV corresponded to carbide [30]. Furthermore, the peak at 285 eV in the C 1s spectrum (Fig. S3b, ESI †) implies the existence of amorphous carbon on the NPs surface, which could also be observed in TEM image (Fig. 1a). Moreover, the G peak at 1600 cm^{-1} and the D peak at 1328 cm^{-1} in the Raman spectrum (Fig. S4, ESI †) indicate graphitic carbon was present on the surface of NPs [31]. The observation was in accordance with previous studies, which also found that amorphous carbon and graphitic carbon were copresent on the iron carbide surface [32, 33]. The magnetic property of Fe_5C_2 NPs was shown in Fig. S5a (ESI †), which demonstrates the NPs contained strong magnetic property with a saturation magnetization value (Ms) of 122 emu/g at 298 K. Fig. S5b (ESI †) and Fig. S5c (ESI †) present the photograph of magnetic separation of the NPs. Fe_5C_2 NPs could be separated easily from solution by using an external magnetic field (within 1 min).

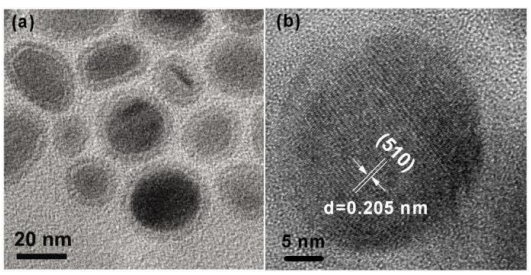

Fig. 1 TEM (a) and HRTEM (b) images of Fe_5C_2 nanoparticles.

Bactericidal activities of Fe_5C_2 NPs

The antibacterial properties of Fe_5C_2 NPs toward two representative bacterial types: Gram-negative *E. coli* and Gram-positive *S. aureus*, both with and without NIR irradiation were investigated and shown in Fig. 2. Moreover, experiments without Fe_5C_2 NPs in physiological saline bacterial solutions of the two cell types both with and without NIR irradiation were also carried out as blank control (Fig. 2). In all control experiments, the cell densities of both *E. coli* and *S. aureus* remained unchanged within the whole processes of disinfection. The observation demonstrated neither sodium chloride solution nor NIR irradiation had toxic effect on the two types of bacterial cells examined in present study. A previous study also found that NIR irradiation have no toxic effect on bacterial cells [25]. The cell densities of both *E. coli* and *S. aureus* with Fe_5C_2 NPs present in the bacterial suspension did not decrease during the disinfection processes without NIR irradiation, indicating that Fe_5C_2 NPs were not effective on the inactivation of bacteria without NIR irradiation. In contrast, under NIR irradiation, the cell densities of both *E. coli* and *S. aureus* in the presence of Fe_5C_2 NPs decreased dramatically within antibacterial duration. Complete disinfection of *E. coli* and *S. aureus* could be reached in 60 min and 150 min, respectively. Clearly, for both cell types, Fe_5C_2 NPs have effective antibacterial activity under NIR irradiation.

It should be noted that carbon nanotube clusters [24] and magnetic reduced graphene oxide functionalized with glutaraldehyde (MRGOGA) [25] have also been demonstrated to contain photothermal antibacterial properties. Specifically, Kim et al. [24] reported that carbon nanotube clusters could inactivate bacterial cells under laser irradiation and complete disinfection of *E. coli* could be observed at 3 J/cm^2. Wu et al. [25] found that MRGOGA could also cause significant damages to bacterial cells upon the NIR irradiation, however, only 0.4% of *S. aureus* and 0.1% of *E. coli* could survive after the photothermal treatment. Although Fe_5C_2 NPs showed similar antibacterial capacity as carbon nanotube clusters, yet it should be pointed out that Fe_5C_2 NPs had the advantage of separation convenience due to the magnetic property. Moreover, comparing with MRGOGA, Fe_5C_2 NPs could complete inactivate both *S. aureus* and *E. coli*, which implied stronger inactivation effect of Fe_5C_2 relative to MRGOGA. These results confirmed that Fe_5C_2 NPs prepared in this study contained strong photothermal bactericidal property and application convenience under NIR irradiation.

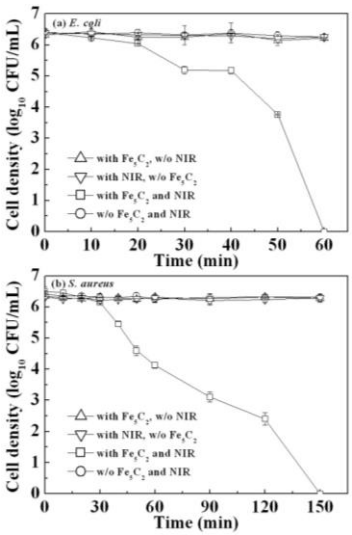

Fig. 2 Inactivation effects of Fe_5C_2 nanoparticles (50 mg/L, pH 6) and NIR irradiation for *E. coli* (a) and *S. aureus* (b). Error bars represent standard deviations from triplicate experiments (n=3).

The complete inactivation duration for *E. coli* (60 min) was shorter than that for *S. aureus* (150 min), indicating that the disinfection effects of Fe_5C_2 NPs with NIR irradiation for Gram-negative *E. coli* were greater than that for Gram-positive *S. aureus*. To quantitatively compare the bactericidal kinetics of Fe_5C_2 NPs for *E. coli* and *S. aureus*, inactivation rate constants for both cell types were determined by using Chick-Watson model [34]. The inactivation rate constants of Fe_5C_2 NPs for *E. coli* and *S. aureus* were found to be 0.249 min^{-1} and 0.101 min^{-1}, respectively. Obviously, the disinfection rate constant of Fe_5C_2 NPs for Gram-negative *E. coli* was larger than those for Gram-positive *S. aureus*. The relatively greater inactivation effects for Gram-negative bacteria relative to Gram-positive bacteria have also been reported previously [26, 35]. For example, Jin et al. [26] found that the inactivation rate constant of Ag_2O/TNBs for Gram-negative *E. coli* was greater than that for Gram-positive *B. subtilis*. The different inactivation rate constants observed for Gram-negative cells and Gram-positive cells could be attributed to the different peptidoglycan structures of cell walls [9]. Comparing to Gram-negative *E. coli*, which has single layer scattered structure of plate mesh, Gram-positive

S. aureus forms a cross-linked and three-dimensional spatial network structure of high mechanical strength, which could resist greater outer environmental stress. As a result, larger inactivation rate constant of Fe_5C_2 NPs for *E. coli* than *S. aureus* was obtained.

Bactericidal mechanisms of Fe_5C_2 NPs

Under NIR irradiation, the temperature of bacterial suspensions without Fe_5C_2 NPs increased from 25 °C to 41 °C with increasing irradiation time (Fig. 3a). However, as stated above, the cell densities of both *E. coli* and *S. aureus* without Fe_5C_2 NPs remained unchanged within disinfection processes when cells were exposed to NIR irradiation, indicating that the increase of temperature to 41 °C within the disinfection processes (60 min) did not inactivate the bacteria. To further testify that the bacteria would not be inactivated at temperature of 41 °C, *E. coli* with initial concentration of 2×10^6 CFU/mL (same as disinfection tests) were exposed to 41 °C for 60 min. At suspension temperature of 41 °C (with water bath), the cell population did not change within 60 min (Fig. 4). The observation further confirmed that increasing temperature of bacterial suspension to 41 °C due to NIR irradiation would not disinfect bacteria.

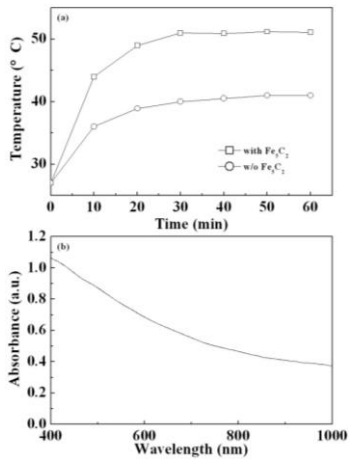

Fig. 3 Temperature changes of bacterial suspension both with and without Fe_5C_2 NPs under NIR irradiation (a) and UV-vis-NIR spectra of Fe_5C_2 NPs (b).

As stated above, without NIR irradiation, Fe_5C_2 NPs did not have any toxic effect towards bacteria. In contrast, under NIR irradiation, Fe_5C_2 NPs exhibited antibacterial activity on both *E. coli* and *S. aureus*. Cleary, the synergistic effect of Fe_5C_2 NPs and NIR irradiation induced the inactivation of bacteria. Previous studies have shown that carbon materials, such as carbon nanotubes [23, 24] and graphene [25], contain photothermal effect, and could convert light energy into heat to destruct cells. The as-synthesized Fe_5C_2 NPs in present study have core-shell structure, and the amorphous shell was mainly constituted of carbon (70.55%). Fe_5C_2 NPs might also contain photothermal effect due to the presence of carbon shell. Thereby, antibacterial effects of Fe_5C_2 NPs might be expected under NIR irradiation. To investigate the light absorption capacity of the fabricated Fe_5C_2 NPs, UV-vis-NIR spectra of 50 mg/L Fe_5C_2 NPs was recorded (Fig. 3b). Similar as that of magnetic reduced graphene oxide functionalized with glutaraldehyde (0.44) [25], Fe_5C_2 NPs exhibited optical absorption from the UV to the NIR region with 0.46 absorbance at 808 nm. Like the reduced graphene oxide, Fe_5C_2 NPs might contain photothermal effect under NIR irradiation. To estimate the photothermal efficiency of the NPs, the temperature evolution profiles of 50 mg/L of Fe_5C_2 NPs solution with NIR irradiation (808 nm, 2.5W/cm^2) as a function of time were recorded (Fig. 3a). With NIR irradiation, the temperature of bacterial suspensions with the copresence of Fe_5C_2 NPs increased as time progressed. Specifically, the temperature increased from 25 °C to 51 °C within 30 min and remained constant (51 °C) thereafter. In comparison to NIR irradiation without Fe_5C_2 NPs, the increase of the temperature with Fe_5C_2 NPs under NIR irradiation was around 1.8 times faster, implied that Fe_5C_2 NPs have excellent photothermal effect (capable of absorbing irradiated light and subsequently release the energy as heat). The fast increase of the mixture temperature to 51 °C might contribute to the inactivation of bacteria.

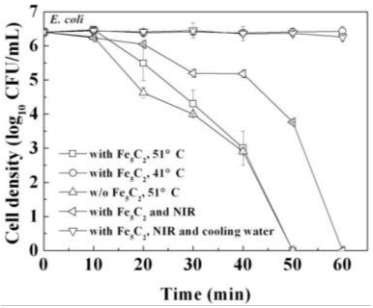

Fig. 4 Inactivation kinetics of *E. coli* under different temperatures (data of "with Fe_5C_2 and NIR" was replotted from Fig. 2). Error bars represent standard deviations from triplicate experiments (n=3).

Previous study [25] found that when the temperature was higher than 50 °C, the enzymes could be denatured and the key intracellular reactions of bacteria would be inhibited. Moreover, proteins and lipids on the cell membrane would also be damaged. As a result, bacteria could be disinfected at temperature above 50 °C. To investigate whether the inactivation of bacteria observed with Fe_5C_2 copresent under NIR irradiation was caused by the increase of temperature in bacterial suspensions to 51 °C, additional experiments were also conducted by exposing *E. coli* suspensions both with and without Fe_5C_2 NPs to hot water at temperature of 51 °C (by employing water bath) yet without NIR irradiation. The results of additional experiments were presented in Fig. 4. Similar as that obtained with Fe_5C_2 NPs in bacterial suspensions with NIR irradiation, the cell densities of *E. coli* dramatically decreased with increasing time in hot water at temperature of 51 °C. Moreover, complete disinfection of bacteria in hot water could be obtained in 50 min. This observation was true both with and without Fe_5C_2 NPs present in the bacterial suspension. As shown in Fig. 2a, at the same initial cell concentration (2×10^6 CFU/mL), complete disinfection of *E. coli* with Fe_5C_2 NPs under NIR irradiation could be reached in 60 min. Clearly, the bacterial inactivation rates in water bath experiments of 51 °C (0.327 min^{-1}) were higher than that with the presence of NPs under NIR irradiation (0.249 min^{-1}). The temperature of bacterial suspension was kept at 51 °C during the whole disinfection experiments for the water bath experiments, yet the temperature of bacterial suspension with Fe_5C_2 NPs under NIR irradiation gradually increased from room temperature (25 °C) to 51°C. As stated above, the inactivation of bacteria could not be observed even at temperature of 41°C (Fig. 4,

circle). Obviously, when the temperature of the suspension with Fe_5C_2 NPs under NIR irradiation exceeded the tolerable temperature of the bacterial cell, the inactivation of bacterial cells could be acquired. The gradual increase of temperature in bacterial suspension to 51°C thus contributed to the slight lower inactivation rates of *E. coli* observed with Fe_5C_2 NPs under NIR irradiation.

To further confirm that the inactivation of bacteria observed with Fe_5C_2 copresent under NIR irradiation was due to the increase of temperature in bacterial suspensions, experiment was conducted by employing cooling water to remove the superfluous heat from bacterial mixture induced by Fe_5C_2 NPs with NIR irradiation. The temperature of the reaction system therefore was maintained at 25 °C (Fig. 4, downtriangle). Interestingly, the cell density unchanged during the whole reaction duration when the temperature of the suspension was kept at 25 °C. The observation indicated that the bacteria could survive with copresence of Fe_5C_2 NPs under NIR irradiation if the temperature of the reaction system was not increased. The results further confirmed that the increase of suspension temperature due to the presence of Fe_5C_2 NPs under NIR irradiation contributed to inactivation of bacteria. Based on the above observations, it is reasonable for us to conclude that the increase of the suspension temperature was a major and possibly the sole contributor to the cell disinfection with the copresence of Fe_5C_2 NPs in suspensions under NIR irradiation.

Furthermore, to examine whether portion of the treated bacterial cells could revive after 60 min of Fe_5C_2 NPs treatment under NIR irradiation, the treated *E.coli* suspensions (with Fe_5C_2 NPs yet without NIR irradiation) were first kept at room temperature (25 °C) for 24 and 48 hours, respectively, and then they were inoculated into the growth medium. After the treated *E.coli* suspension was kept at room temperature for 24 h, the cell resurrection densities were found to be 20 CFU/mL, indicating that a small portion of cells (0.001%) were revived. The same cell resurrection rates (20 CFU/mL) were acquired after the treated cell suspension was kept at 25 °C for 48 h. Increasing the store time for the treated cells at room temperature did not change their revived rates. Although a small portion of cells revived after disinfection with Fe_5C_2 NPs treatment under NIR irradiation for 60 min, the revived rate relative to the initial cell density (2×10^6 CFU/mL) was only 0.001%, which implied that about 5-log decrease of cell densities could still be obtained after exposing cells to Fe_5C_2 NPs with NIR irradiation for 60 min. Increasing the disinfection time would decrease the revived rate of treated cells. When *E.coli* cells were disinfected with Fe_5C_2 NPs under NIR irradiation for around 2 hour, none of the cells was found to revive after the treated cells were stored at room temperature for 24 hours.

ESEM images of *E. coli* cell at different Fe_5C_2 NPs treatment time under NIR irradiation were employed to investigate the morphology changes of the bacterial cell by the photothermal effect (Fig. 5). *E. coli* cell morphology gradually changed from full and smooth cell to shrivelled and withered cell. At the beginning of the treatment, the *E. coli* cell had an intact cell structure with well-stacked cell wall (Fig. 5a). While the cell morphology gradually changed after 30 min and the cell begun to shrivel (Fig. 5b), indicating that the cell wall and membrane were partly damaged. When the treatment time was increased to 60 min, *E. coli* cell was deformed to be cataplastic and the interior components of the cell leaked out, which resulted the death of the bacteria (Fig. 5c). This observation is similar with previous studies that reactive species could attack the cell wall and membrane, destroying the membrane integrity and leading to the leakage of cytoplasm [36-38].

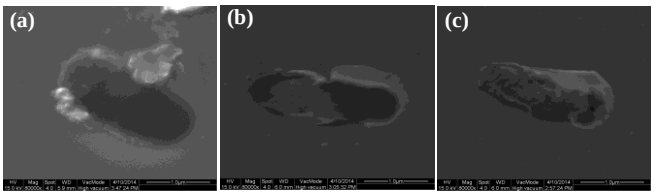

Fig. 5 ESEM images of *E. coli* cell at different Fe_5C_2 NPs treatment time under NIR irradiation (a: 15 min; b: 30 min; c: 60 min).

Effect of HA on bactericidal activities of Fe_5C_2 NPs

NOM is ubiquitous in the aquatic environment. Humic acid (HA) is an important constituent of NOM and has been frequently employed to model NOM [11, 15]. The effect of HA on the photothermal disinfection of Fe_5C_2 NPs under NIR irradiation was also explored by adding different amounts of HA into the reaction system, and the results were shown in Fig. 6. The addition of HA into cell suspensions could inhibit the antibacterial performance of Fe_5C_2 NPs, and the survived bacterial density increase from 0 at 2 mg/L of HA to 3.2-log at 10 mg/L of HA. The decrease of the bactericidal property of Fe_5C_2 NPs in the presence of HA might be due to the adsorption of HA onto the surface of the NPs, which could in turn inhibit the NIR adsorption capacity of the NPs and decrease the photothermal effect. Previous study [11] also found that HA could be adsorbed by multi-walled carbon nanotubes (MWCNTs) and then decreased the antibacterial property of Ag-MWCNTs. To determine whether the presence of HA could inhibit the NIR adsorption capacity of the Fe_5C_2 NPs and decrease the photothermal effect, the temperature variations of Fe_5C_2 nanoparticles suspension in the presence of 10 mg/L of HA under the NIR irradiation was measured and the results were shown in Fig. S6. With the presence of 10 mg/L HA, the temperature of Fe_5C_2 nanoparticles suspension gradually increased from 25 °C to a plateau of 46° C after 50 minutes of NIR irradiation. Whereas, as stated above, the temperature of Fe_5C_2 suspensions rapidly increased from 25 °C to 51 °C within 30 min and remained constant (51 °C) thereafter in the absence of HA (Fig. 3a). Obviously, the presence of HA in suspensions could inhibit the NIR absorption capacity of Fe_5C_2 NPs and decrease the photothermal effect, resulting in the decrease of antibacterial property of Fe_5C_2 NPs.

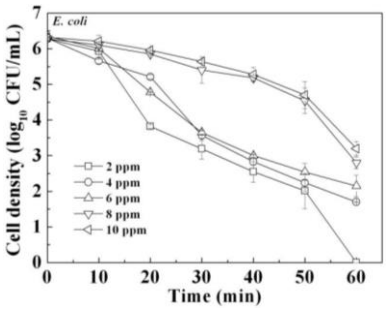

Fig. 6 Effect of humic acid on the antibacterial property of Fe_5C_2 NPs under NIR irradiation. Error bars represent standard deviations from triplicate experiments (n=3).

However, it should be noted that 3-log decrease of *E. coli* cell density could be reached even in the presence of 10 mg/L of HA, which means that 99.9% of the bacterial cells

could be inactivated at HA concentration as high as 10 mg/L. The typical concentration of HA in aquatic environment is commonly below 10 mg/L [39]. In case of coexistence of humic acid at elevated concentrations (e.g. ~10 mg/L), the disinfection rates could be enhanced by appropriately prolonging the reaction time. For example, when the reaction time was prolonged to 90 min, complete disinfection of *E. coli* cells could also be obtained in the presence of 10 mg/L of HA.

Reusability estimation

The reusability of Fe_5C_2 NPs for photothermal disinfection treatment was investigated with five successive cyclic experiments under NIR irradiation. It should be noted that 75% of ethanol was employed to remove the treated bacteria after each cycle, and then Fe_5C_2 NPs were washed with physiological saline solution for three times before the next cycle. During the ethanol treatment and saline wash processes, a magnet was put on the sidewall of the beaker to prevent the loss of the Fe_5C_2 NPs. Five consecutive antibacterial experiments were conducted and the results were shown in Fig. 7. Complete disinfections of *E. coli* were observed in 60 min treatment for all the five consecutive experiments, implied that the photothermal disinfection activity of Fe_5C_2 NPs under NIR irradiation did not decrease with increasing the recycle and reuse times. The results demonstrated that Fe_5C_2 NPs can be used as effective and stable photothermal antibacterial material under NIR irradiation.

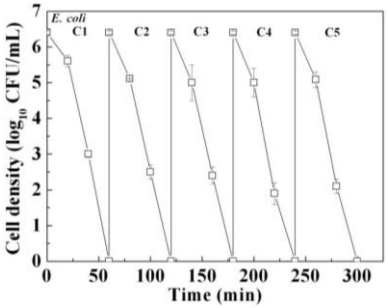

Fig. 7 Reusability of Fe_5C_2 NPs under NIR irradiation (C refers to reuse cycle). Error bars represent standard deviations from triplicate experiments (n=3).

Conclusions

Fe_5C_2 nanoparticles with diameter of 20 nm were synthesized through a facile route and showed strong magnetic property (*Ms*=122 emu/g at 298 K). Moreover, Fe_5C_2 nanoparticles exhibited excellent photothermal effect and antibacterial capability under NIR irradiation. 2×10^6 CFU/mL of *E. coli* and *S. aureus* cells could be inactivated in the presence of 50 mg/L of Fe_5C_2 NPs under NIR irradiation in 60 min and 150 min, respectively. Although portion of cells (0.001%) revived after they were kept at room temperature for 24 h, more than 5-log decrease of cell density could still be obtained. Moreover, none of treated cells could revive with increasing the disinfection time to ~2 hour. HA could inhibit the photothermal disinfection property of Fe_5C_2, prolonging the treatment time yet could ensure the complete inactivation of the bacterial cells. Moreover, Fe_5C_2 NPs contained excellent reusability, and high antibacterial property could be maintained even after five consecutive cycles. The antibacterial mechanism of Fe_5C_2 NPs could be attributed to the photothermal effect of Fe_5C_2 NPs under NIR irradiation, which resulted in the increase of the temperature of bacterial suspension and lead to the death of bacteria. With the efficient antibacterial activity from photothermal effect and the strong absorption property for UV to NIR region light, Fe_5C_2 might be used as a novel photothermal sterilization material under normal solar light. Efforts should also be taken to explore the real application of Fe_5C_2 nanoparticles and extend their application potentials in the future work.

Acknowledgements

This work was supported by the National Natural Science Foundation of China under Grant No. 21177002 and 21377006, also partly by the program for New Century Excellent Talents in University under grant No. NCET-13-0010 and Specialized Research Fund for the Doctoral Program of Higher Education, Ministry of Education of China under Grant No. 20100001110034. We acknowledge the two anonymous reviewers for their valuable help in the review and revision process.

Notes and references

[a] The Key Laboratory of Water and Sediment Sciences, Ministry of Education; College of Environmental Sciences and Engineering, Peking University, Beijing, 100871, P. R. China.
[b] Currently at Huadian Electric Power Research Institute, Hangzhou, 310030, China.
[c] Department of Advanced Materials and Nanotechnology, College of Engineering, Peking University, Beijing, 100871, P. R. China.

† Electronic Supplementary Information (ESI) available: XRD patterns, XPS spectra of Fe_5C_2 nanoparticles; XPS spectra of Fe 2p (a) and C 1s (b) of Fe_5C_2 nanoparticles; Raman spectra of Fe_5C_2 nanoparticles; Magnetism curve (a) and magnetic separation photo (b) of Fe_5C_2 nanoparticles. See DOI: 10.1039/b000000x/

1 WHO, Emerging Issues in Water and Infectious Disease, in: W.H. Organization (Ed.), Geneva, 2003, pp. 1-22.
2 A. M. Shannon, W. P. Bohn, M. Elimelech, G. J. Georgiadis, J. B. Marinas, M. A. Mayes, *Nature*, 2008, 452, 301-310.
3 W. S. Krasner, S. H. Weinberg, D. S. Richardson, J. S. Pastor, R. Chinn, J. M. Sclimenti, D. G. Onstad, D. A. Thruston, J. R., *Environ.Sci.Technol.*, 2006, 40, 7175-7185.
4 Q. Li, S. Mahendra, D. Y. Lyon, L. Brunet, M. V. Liga, D. Li, P. J. J. Alvarez, *Water Res.*, 2008, 42, 4591-4602.
5 A. Erkan, U. Bakir, G. Karakas, *J. Photochem. Photobiol. A*, 2006, 184, 313-321.
6 M. Mahmoudi, Serpooshan, V., *Acs Nano*, 2012, 6, 2656-2664.
7 K. K. T. Kumarasamy, M. A. Walsh, T. R. Bagaria, J. Butt, F. Balakrishnan, R. Chaudhary, U. Doumith, M. Giske, C. G. Giske, S. Irfan, et al., *Lancet Infect. Dis.*, 2010, 10, 597-602.
8 Z. Xiong, J. Ma, W. J. Ng, T. D. Waite, X.S. Zhao, *Water Res.*, 2011, 45, 2095-2103.
9 Q. Bao, D. Zhang, P. Qi, *J. Colloid Interface Sci.*, 2011, 360, 463-470.
10 L. Liu, Z. Liu, H. Bai, D. D. Sun, *Water Res.*, 2012, 46, 1101-1112.
11 R. Su, Y. Jin, Y. Liu, M. Tong, H. Kim, *Colloids Surf. B*, 2013, 104, 1[33]–139.
12 Y. Li, W. Zhang, J. Niu, Y. Chen, *Acs Nano*, 2012, 6, 5164-5173.
13 Y. Li, J. Niu, W. Zhang, L. Zhang, E. Shang, *Langmuir*, 2014, 30, 2852-2862.
14 W. J. Chen, P. J. Tsai, Y. C. Chen, *Small*, 4, 485-491.

15 Y. Jin, F. Liu, C. Shan, M. Tong, Y. Hou, Water Res., 2014, 50, 124-134.
16 W. J. Chen, Y. C. Chen, *Nanomedicine*-UK, 2010, 5, 1585-1593.
17 L. Bromberg, E. P. Chang, T. A. Hatton, A. Concheiro, B. Magarinos, C. Alvarez-Lorenzo, *Langmuir*, 21, 420-429.
18 M. Sureshkumar, D. Y. Siswanto, C.-K. Lee, *J. Mater. Chem.*, 2010, 33, 6948-6955.
19 A. Alonso, N. Vigue´s, X. Munoz-Berbel, J. Macanas, M. Munoz, J. Mas, D. N. Muraviev, *Chem. Commun.*, 2011, 47, 10464-10466.
20 R. Prucek, J. Tucek, M. Kilianová, A. Panácek, L. Kvítek, J. Filip, M. Kolár, K. Tománková, R. Zboril, *Biomaterials*, 2011, 32, 4704-4713.
21 C. Yang, H. Zhao, Y. Hou, D. Ma, *J. Am. Chem. Soc.*, 2012, 134, 15814–15821.
22 Y. Jin, Liu, F., Tong, M., Hou, Y., *J. Hazard. Mater.*, 2012, 227-228, 461-468.
23 N. W. S. Kam, O'Connell, M., Wisdom, J. A., Dai, H., *Proc. Natl. Acad. Sci.* USA, 2005, 102, 11600-11605
24 J. W. Kim, Shashkov, E. V., Galanzha, E. I., Kotagiri, N., Zharov, V. P., *Lasers Surg. Med.*, 2007, 39, 622-634.
25 M.-C. Wu, Deokar, A. R., Liao, J.-H., Shih, P.-Y., Ling, Y.-C., *Acs Nano*, 2013, 7, 1281-1290.
26 Y. Jin, Dai, Z., Liu, F., Kim, H., Tong, M., Hou, Y., *Water Res.*, 2013, 47, 1837-1847.
27 A. Franchi, O'Melia, C. R., *Environ. Sci. Technol.*, 2003, 37, 1122-1129.
28 K. L. Chen and M. Elimelich, *Langmuir*, 2006, 22, 10994-11001.
29 N. B. Saleh, L. D. Pfefferle, and M. Elimelich, *Environ. Sci. Technol.* 2008, 42, 7963–7969.
30 C.-J. Jia, L.-D. Sun, F. Luo, X.-D. Han, L. J. Heyderman, Z.-G. Yan, C.-H. Yan, K. Zheng, Z. Zhang, M. Takano, N. Hayashi, M. Eltschka, M. Kla¨ui, U. Ru¨diger, T. Kasama, L. Cervera-Gontard, R. E. Dunin-Borkowski, G. Tzvetkov, J. Raabe, *J. Am. Chem. Soc.*, 2008, 130, 16968–16977.
31 A. C. Ferrari, J. C. Meyer, V. Scardaci, C. Casiraghi, M. Lazzeri, F. Mauri, S. Piscanec, D. Jiang, K. S. Novoselov, S. Roth, A.K. Geim, *Phys. Rev. Lett.*, 2006, 97, 187401.
32 N. B. Jackson, A. K. Datye, L. Mansker, R. J. O'Brien, B. H. Davis, *Stud. Surf. Sci. Catal.*, 1997, 111, 501–516.
33 J. Xu , H. C. Bartholomew, J. Phys. Chem. B, 2005, 109, 2392-2403.
34 F. Chen, X. Yang, F. Xu, Q. Wu, Y. Zhang, *Environ. Sci. Technol.*, 2009, 43, 1180-1184.
35 H. Li, X. Zhu, J. Ni, *Electrochim. Acta*, 2011, 56, 9789-9796.
36 M. Cho, H. Chung, W. Choi, J. Yoon, *Appl. Environ. Microbiol.*, 2005, 71, 270-275.
37 L. S. Zhang, K. H. Wong, H. Y. Yip, C. Hu, C. J. Yu, C. Y. Chan, P. K. Wong, *Environ. Sci. Technol.*, 2010, 44, 1392-1398.
38 Y. Chen, A. Lu, L. S. Zhang, Y. Y. Ho, H. Zhao, T. An, P. K. Wong, *Environ. Sci. Technol.*, 2011, 45, 5689-5695.
39 U. Olofsson, B. Allard, Complexes of Actinides with Naturally Occurring Organic Substances: Literature Survey, in, Svensk Kärnbränsleförsörjning, Goteborg, 1983, pp. 54.